Wave transmission: spectral changes and its effects on run-up and overtopping

J.W. van der Meer[1], H.J. Regeling[2] and J.P. de Waal[3]

Introduction

Most research work on wave transmission over low-crested structures has been concentrated on establishing the wave transmission coefficient, i.e. the ratio between transmitted and incident significant wave height. It is clear that such structures decrease the wave height, but there is more!

Goda (1985), Tanimoto et al. (1987), Raichlen et al. (1992) and Van der Meer (1990) all conclude that also the mean period reduces to 0.4-1.0 of the incident mean period. The conclusion is that overtopping generates more waves. Further, Raichlen et al. (1992) and Lee (1994) give examples of measured spectra of transmitted waves. Both examples show the peak of the spectrum similar to the incident spectrum, but with much more energy at the higher frequencies.

A good estimation of the wave height in front of a structure is required for design or assessment of such a structure. But also wave period and sometimes spectral shape may have influence on the design. Wave run-up, for example, depends largely on the wave period. In order to establish the required dike height for acceptable run-up, both wave height and period should be known. In situations where a low-crested structure in front of such a dike gives some protection, wave period and spectral changes should be studied.

A local situation in the Netherlands was the reason for the research presented in this paper. Figure 1 gives a schematised layout. A large lake is situated on the west side (left side in the figure) and NW wind may generate waves up to a significant wave height of over 2 m. The dikes on the eastern side are partly protected by a system of various low-crested structures or dams, including some openings.

[1]Infram, PO Box 81, 3890 AB, Zeewolde, the Netherlands;
jentsje.vandermeer@infram.nl;
[2]Public Works Department, IJsselmeer District, the Netherlands;
e.regeling@rdij.rws.minvenw.nl;
[3]Public Works Department, RIZA, the Netherlands; h.dwaal@riza.rws.minvenw.nl

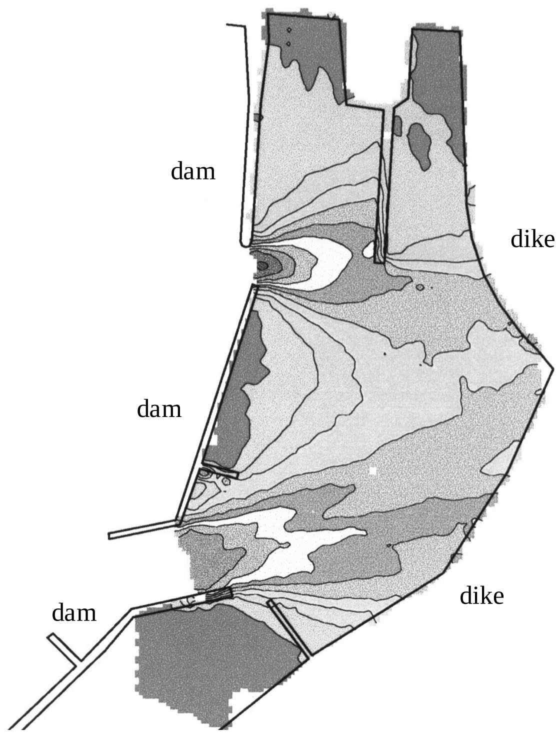

Figure 1. Schematised layout of dikes protected by low-crested structures or dams. The figure shows the results of wave penetration through two openings. The lake is on the left side of the figure.

The figure shows the results of a calculation on wave penetration. Such calculations were performed by Alkyon. Besides wave penetration, wave transmission is generated over the low-crested dams. The area is about 1 km by 2.5 km. This means that with a fetch of more than 1 km also locally generated (short) waves will be present during extreme conditions. The wave climate in front of the dikes can be described as a combination of wave penetration, wave transmission and locally generated wind waves. This paper deals with wave transmission only, but the effect on the total wave climate is discussed at the end.

Model tests

A model investigation was performed in a wave flume of Delft Hydraulics and the results were analysed by Infram. The model scale was 1:15 and all results are given in prototype values. In total five different structures were tested: smooth (asphalt) with various crest widths, smooth covered with rock and a very wide caisson. Figures 2-6 give the cross-sections of these structures. Dams 1 and 2 are similar, except that for dam 2 a 0.75 m thick rock layer of 60-300 kg rock was placed on top of the asphalt slope. All slopes were 1:4, both seaward and landward of the crest.

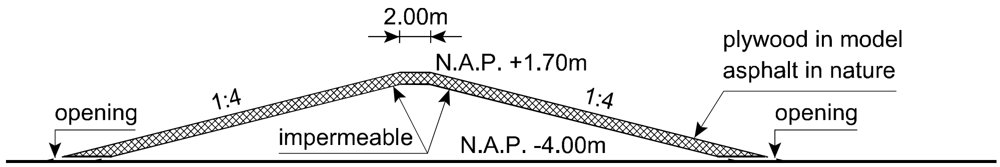

Figure 2. Dam 1. Smooth 1:4 slopes with crest width of 2 m

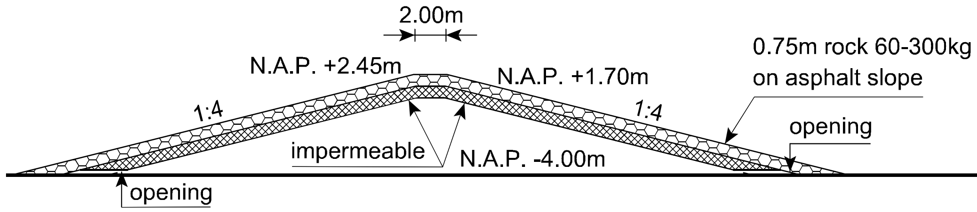

Figure 3. Dam 2. As dam 1, but covered with 60-300 kg rock

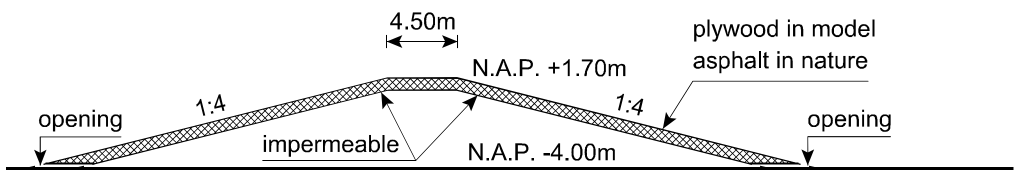

Figure 4. Dam 3. Smooth 1:4 slopes with crest width of 4.5 m

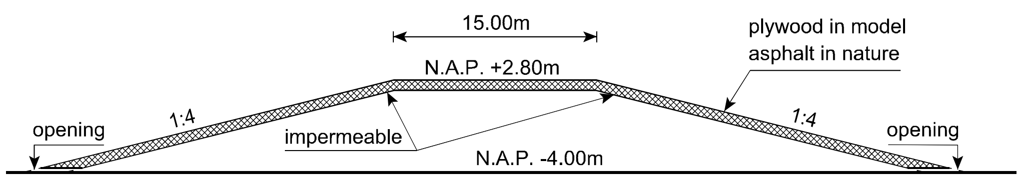

Figure 5. Dam 4. Smooth 1:4 slopes with crest width of 15 m

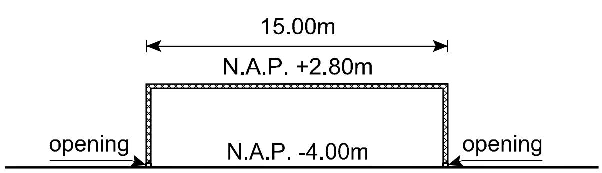

Figure 6. Low-crested caisson with wide crest

The main difference between dams 1, 3 and 4 is the crest width. The models were made of plywood and an opening was left near the bottom of the flume in order to maintain the same water level in front and behind the model. Various wave gauges measured the incident and reflected waves and the wave transmission. The model was placed in the middle of the flume with a spending 1:10 beach at the end.

In total 28 tests were performed. The water depth ranged between 4.5 and 7 m and the wave heights between H_{m0}=1.3-2.2 m with peak periods between T_p=5-7 s. Actually, the wave steepness was kept constant at s_{op}=0.03. The relative crest height ranged between R_c/H_{m0}=0-1.0, which means low-crested structures with the crest just above the still water level. The wave transmission coefficients measured varied between K_t=0-0.4. Table 1 gives the main results.

Table 1. Main test results

test	type	B	h_c	swl	incident H_{m0}	incident T_p	incident T_m	C_r	transmitted H_{m0}	transmitted T_p	transmitted T_m	K_t
		m	m	m	m	s	s		m	s	s	
1	dam 1	2	1.7	0.30	1.29	5.24	4.34	0.216	0.08	6.97	3.84	0.060
2	dam 1	2	1.7	0.60	1.46	5.70	4.61	0.233	0.26	6.68	3.37	0.178
3	dam 1	2	1.7	0.90	1.66	5.95	4.91	0.245	0.46	6.10	3.37	0.275
4	dam 1	2	1.7	1.20	1.83	6.37	5.13	0.244	0.61	6.62	3.41	0.335
5	dam 1	2	1.7	1.60	2.02	6.71	5.38	0.217	0.81	6.80	3.75	0.403
6	dam 2	2.5	2.45	1.71	1.94	6.44	5.23	0.204	0.14	7.28	3.03	0.074
7	dam 2	2.5	2.45	1.80	2.10	6.76	5.41	0.196	0.30	6.94	3.14	0.145
8	dam 2	3.5	2.6	1.10	1.72	6.05	4.92	0.187	0.04	6.72	6.15	0.024
9	dam 2	3.5	2.6	1.27	1.89	6.37	5.09	0.210	0.06	6.90	5.14	0.029
10	dam 2	3.5	2.6	1.67	1.97	6.71	5.41	0.202	0.16	6.98	3.41	0.080
11	dam 3	4.5	1.7	0.30	1.34	5.29	4.31	0.206	0.07	7.00	3.30	0.056
12	dam 3	4.5	1.7	0.60	1.53	5.71	4.60	0.235	0.25	6.87	3.15	0.167
13	dam 3	4.5	1.7	0.90	1.72	6.06	4.88	0.244	0.44	6.40	3.28	0.259
14	dam 3	4.5	1.7	1.20	1.90	6.45	5.13	0.238	0.61	6.62	3.39	0.322
14a	PM	4.5	1.7	1.20	1.87	6.62	4.81	0.244	0.57	7.06	3.32	0.304
15	dam 3	4.5	1.7	1.60	2.07	6.67	5.39	0.213	0.82	6.94	3.60	0.396
16	dam 4	15	2.8	1.20	1.91	6.41	5.09	0.255	0.19	8.56	2.85	0.102
17	dam 4	15	2.8	1.60	2.07	6.65	5.34	0.264	0.39	7.94	3.02	0.188
18	dam 4	15	2.8	0.90	1.75	5.99	4.90	0.225	0.09	6.94	3.43	0.052
18a	closed	15	2.8	0.90	1.75	5.99	4.87	0.242	0.10	7.04	6.38	0.059
19	dam 4	15	2.8	2.20	2.18	6.70	5.45	0.220	0.60	7.34	3.25	0.273
20	dam 4	15	2.8	2.20	2.02	6.35	5.25	0.212	0.51	7.09	3.13	0.254
20a	dam 4	15	2.8	3.00	2.01	6.33	5.24	0.148	0.66	6.62	3.39	0.326
21	caisson	20	1.5	0.83	1.24	4.00	3.59	0.766	0.11	4.25	3.37	0.085
22	caisson	20	1.5	0.78	1.47	5.68	4.67	0.749	0.20	5.74	4.30	0.133
23	caisson	20	1.5	1.17	0.59	6.37	5.28	0.837				0.000
24	caisson	20	1.5	1.14	1.04	3.99	3.51	0.754	0.09	4.38	3.40	0.089
25	caisson	20	1.5	1.41	0.84	6.64	5.52	0.755	0.13	6.55	3.47	0.149

In Table 1, B= the crest width, h_c = the crest height relative to NAP (chart datum), swl is the water level relative to NAP, H_{m0} = the incident spectral wave height, T_p = the peak period, T_m = the mean period $\sqrt{m_0 / m_2}$, C_r = the reflection coefficient and K_t = the wave transmission coefficient $\sqrt{m_0 t / m_0 i}$ with t and i respectively for transmitted and incident values.

Analysis of results

Wave transmission coefficients. The transmission coefficients are not the main item of this paper, but may be valuable for other applications. They will be treated briefly. The main results are shown in Figure 7 where the wave transmission coefficient K_t is given as a function of the relative crest height R_c/H_{m0}. A few conclusions can be drawn.

First of all there is very little difference between the results of dams 1, 3 and 4, which only differ in crest width. For rubble mound structures a large influence of crest width is present, see for instance Van der Meer and Daemen (1994). The small influence for the tested dams can be explained by the way of wave breaking and the smooth surface. Due to the gentle slope of 1:4 waves break and the up-rushing wave tongue jumps over the smooth crest. In this process the width of the crest plays hardly a role as the surface is smooth without friction or permeability to reduce energy.

The difference in results between dam 1 and 2 is large. The permeable rock layer reduces the transmission by about a constant value of 0.15 and this for the same *relative* crest height!

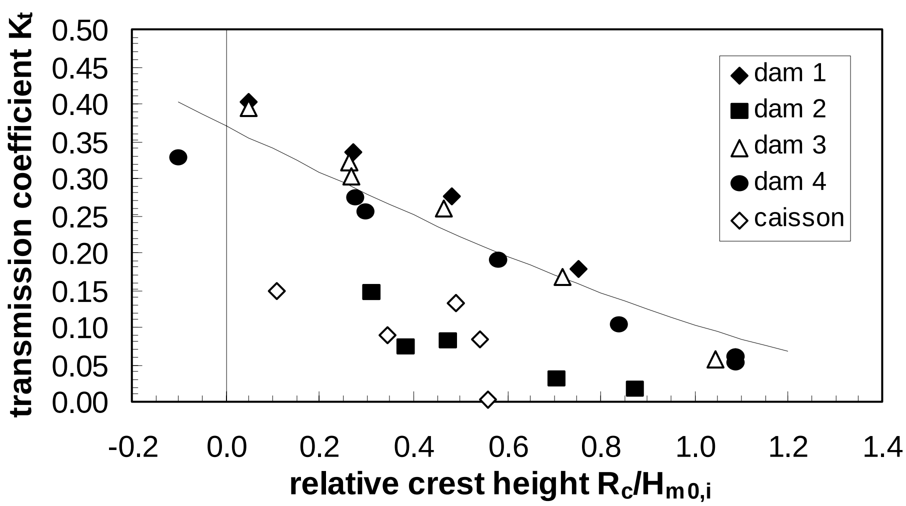

Figure 7. Wave transmission for the 5 tested structures

An efficient formula for fitting wave transmission results is described by Goda (1969). The formula is governed by two fitting coefficients α and β:

$$\frac{R_c}{H_i} \le -\alpha - \beta : \qquad K_t = 1$$

$$-\alpha - \beta \le \frac{R_c}{H_i} \le \alpha - \beta : \qquad K_t = \frac{1}{2}\left(1 - \sin\left(\frac{\pi}{2}\frac{\frac{R_c}{H_i} + \beta}{\alpha}\right)\right) \qquad (1)$$

$$\frac{R_c}{H_i} \ge \alpha - \beta \qquad K_t = 0$$

The fitted formula for the smooth dams is shown in Figure 7. Here α=2.4 and β=0.4. For dam 2 (rock layer) and the wide and low caisson the coefficients were α=1.6 and β=0.5, respectively α=1.8 and β=0.6.

Wave spectra. In most cases Jonswap spectra were generated in the flume. Only in test 14a a wider Pierson Moskowitz spectrum was used. Figure 8 shows three spectra which were measured offshore. The wave heights were respectively 1.34 m, 1.72 m and 2.07 m.

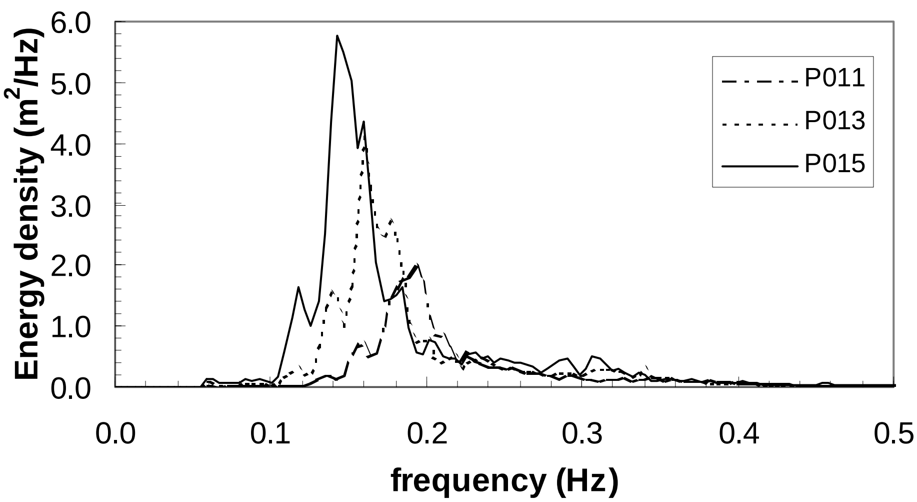

Figure 8. Example of measured spectra offshore

In Figure 9 two spectra are shown which are characteristic for transmitted spectra. The transmitted wave heights here were 0.61 m and 0.81 m, respectively. There is still a clear peak, sometimes even more narrow than the incident spectrum, but there is also energy present for larger frequencies. This energy is fairly constant over a wide frequency range. A more thorough analysis showed that this range was in average close to 1.5 f_p to 3.5 f_p, where f_p is the peak frequency.

Peak period. The transmitted spectra showed that the peak period remained more or less the same. In order to analyse this in a more objective way the ratio between peak

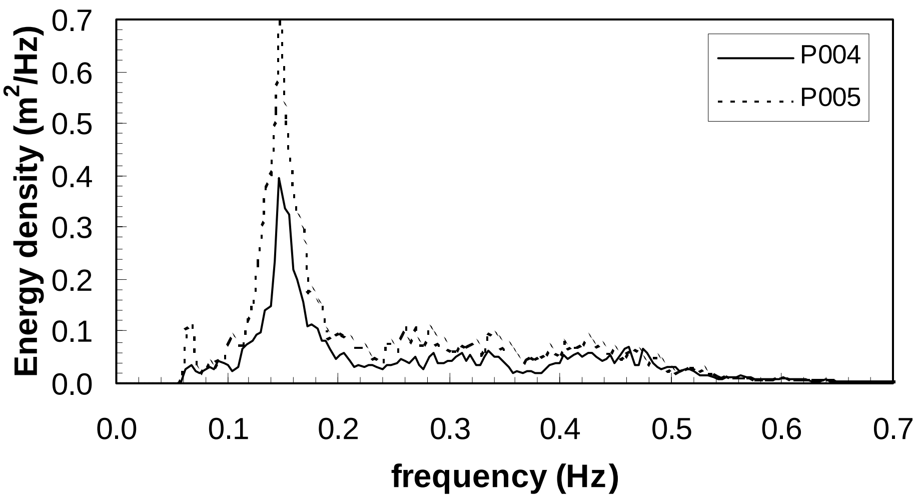

Figure 9. Example of measured transmitted spectra

periods transmitted and offshore was calculated for each test. In general there are two obvious ways to relate these period ratios to an other parameter: as a function of the wave transmission coefficient K_t or the relative crest height, R_c/H_{m0}. The results will be more or less similar as a smaller transmission coefficient often means a larger crest height and vice versa. The full analysis was performed with both parameters, but here only the transmission coefficient will be used. The results were more clear for this parameter.

Figure 10 shows the period ratio T_pt/T_pi as a function of the wave transmission coefficient K_t. The ratio is close to 1, especially for transmission coefficients larger than K_t=0.2. For very small transmission coefficients there is a tendency that the peak period increases after transmission.

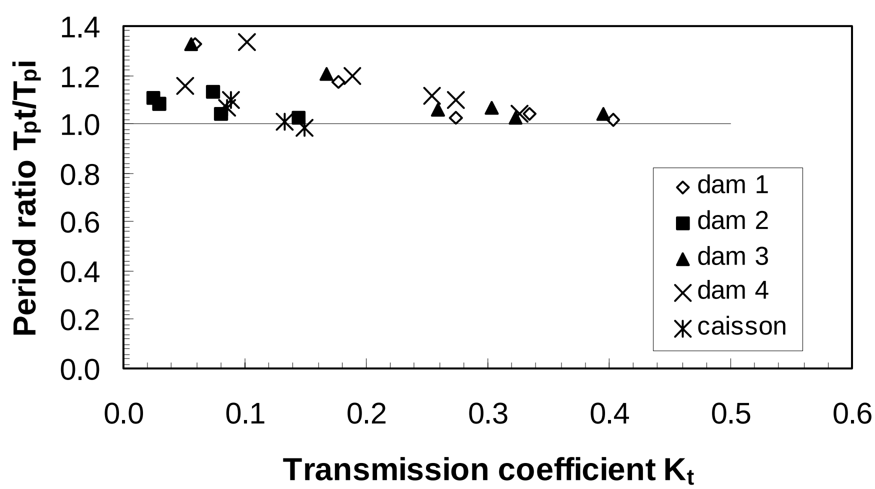

Figure 10. Ratio of peak period transmitted/offshore as a function of transmission

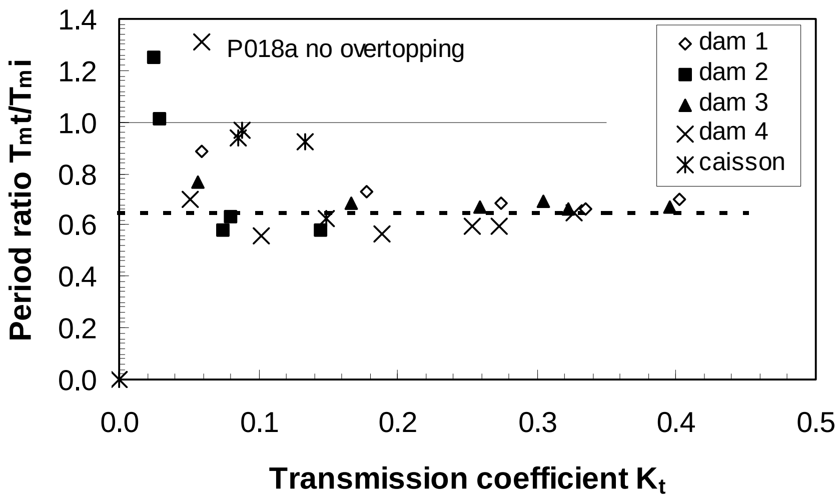

Figure 11. Ratio of mean period transmitted/offshore as function of transmission

The mean period was defined as $T_{m02}=\sqrt{m_0/m_2}$. The ratio of this mean period for transmitted and offshore locations is given in Figure 11. From this figure it is clear that the mean period decreases due to overtopping or transmission. Actually, the waves break on the smooth slope and jump over the crest into the water behind the structure. This jump often will create two waves instead of one and this will decrease the mean period, not the peak period.

Only a few tests showed an increase which was only for very small transmission coefficients. During test 18a there was no wave transmission over the dam as this was blocked in the flume by a vertical plate on top of the crest. The wave transmission measured was due to small transmission underneath the structure through the openings that were created in order to maintain the same water level in front and behind the structure. In average the mean period reduced to about 0.65 of the period offshore, certainly for $K_t>0.15$.

Spectral width. If peak periods, due to transmission or overtopping, remain more or less the same, but mean periods decrease then this is a strong indication that the spectral width also changes. Van Vledder (1992) gives a good overall view of wave group statistics and spectral parameters. The spectral narrowness parameter κ can be calculated both in time and frequency domain, resulting in κ(f) and κ(t). One is referred to Van Vledder (1992) for definitions. A general meaning is as follows:

Type of spectrum	*κ(f)*	*κ(t)*
very narrow	0.8-0.9	0.8-0.9
Jonswap	0.5-0.7	0.5-0.8
Pierson Moskowitz	0.4-0.6	0.5-0.6
wide	0.2-0.4	0.4-0.5
bi-modal	0.2-0.4	0.4-0.5

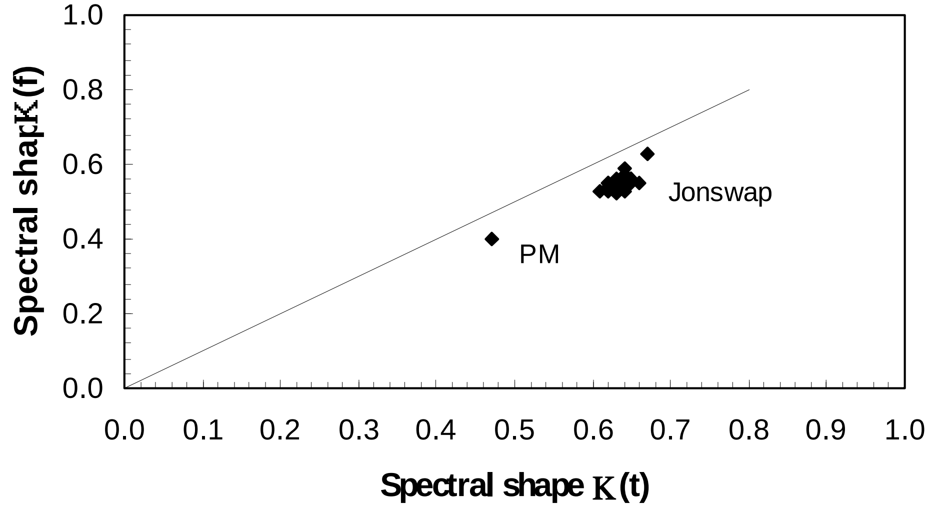

Figure 12. Spectral narrowness parameters measured offshore

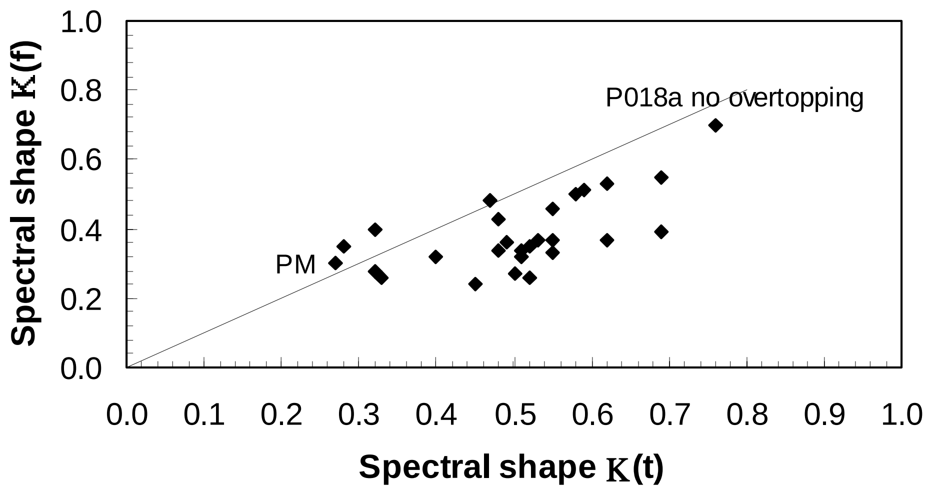

Figure 13. Spectral narrowness parameters measured after transmission

Figure 12 shows both measured spectral narrowness parameters for the offshore location. It is very clear that all Jonswap spectra have the same spectral narrowness and that the only test with a Pierson Moskowitz spectrum is much wider, resulting in a smaller value for the narrowness parameter. A similar graph is shown in Figure 13, but now for the wave spectra after transmission. Now the narrowness is much smaller, indicating that the spectrum is much wider. The smallest value for the Pierson Moskowitz spectrum is still the smallest after transmission. The test without overtopping, but with some energy passing underneath the structure in the flume, shows a very narrow spectrum.

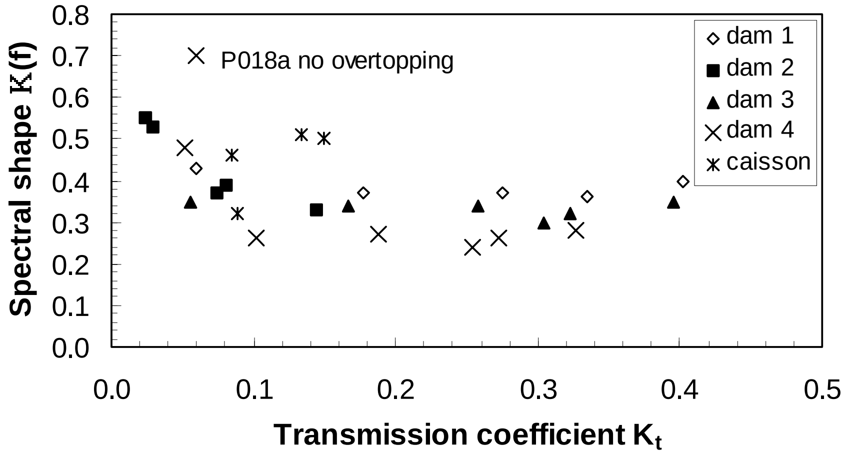

Figure 14. Spectral narrowness after transmission as a function of K_t

Figure 14 shows the spectral narrowness parameter κ(f) as a function of the transmission coefficient K_t. For transmission coefficients K_t>0.15 it can be concluded that wide spectra are generated by overtopping giving spectral narrowness values of κ(f)=0.25-0.35.

Energy shift. On the basis of Figure 9 it was concluded that energy was shifted from the peak frequency to higher frequencies and that a fairly constant level of energy was present between 1.5 f_p and 3.5 f_p. The value of 1.5 f_p can be considered as the boundary between "high" and "low" frequency energy. From the transmitted spectra the energy m_0 for frequencies larger than 1,5 f_p was calculated. In Figure 15 this energy is compared with the total energy in the transmitted spectrum.

A clear conclusion can be drawn from this graph: for transmission coefficients K_t>0.15 a constant ratio is found of 0.4 (the line in the graph).

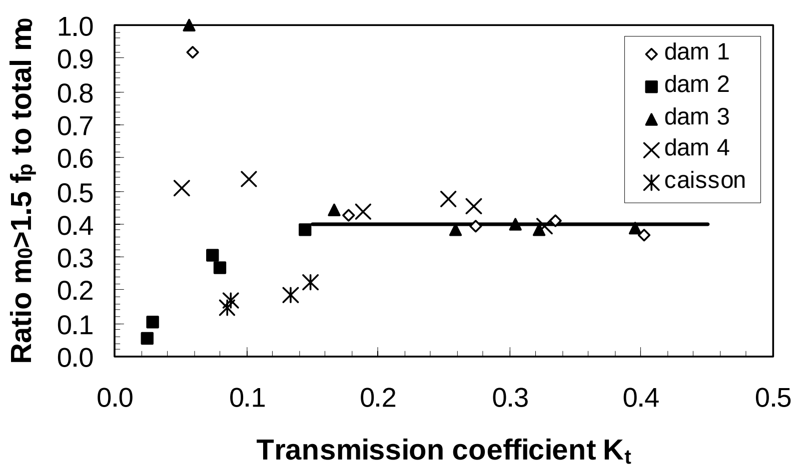

Figure 15. Energy for frequencies larger than1.5 f_p related to total energy m_0

Main conclusions based on the analysis of the tests

The analysis of results of the model tests as described above gives the following conclusions:

- the peak period remains more or less constant
- for wave transmission coefficients K_t > 0.15-0.20 clear trends are found. For lower values the picture is more diffuse and difficult to describe
- for K_t > 0.20 the peak period may increase by not more than 10%
- for K_t > 0.15 the mean period decreases to 0.65 of the incident mean period
- for K_t > 0.15 the spectral narrowness parameter κ_f becomes 0.25-0.35 which indicates a very wide spectrum
- for K_t > 0.15 about 40% of the total transmitted energy is present at the higher frequencies of the spectrum, more specifically between 1.5 f_p and 3.5 f_p.

Method for description of the transmitted spectrum

Conclusions above can be used to develop a prediction method for the spectral shape after wave overtopping or transmission. The basis for this method is the incident spectrum (shape and energy) and the measured or calculated transmission coefficient K_t. For the structures considered here the transmission coefficients in Table 1 or in Figure 7 can be used. The energy of the transmitted spectrum can be calculated by:

$$m_{0,t} = K_t^2 \, m_{0,i} = (0.25 \, K_t \, H_{m0,i})^2 \qquad (2)$$

where t and i stand for transmitted and incident, respectively. The spectral shape remains the same, see Figure 16. In this graph a Pierson Moskowitz spectrum has been assumed with a wave peak period of 6 s. The transmission coefficient was considered to be K_t=0.3, which gives the transmitted spectrum.

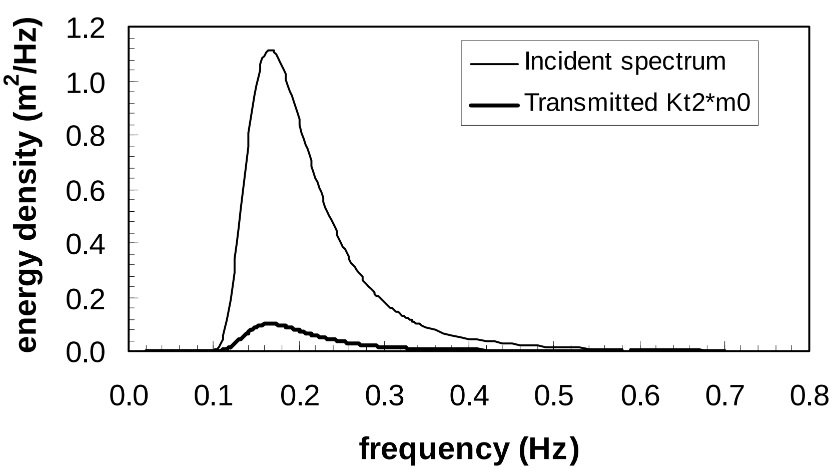

Figure 16. Incident and calculated spectrum, based on the transmission coefficient

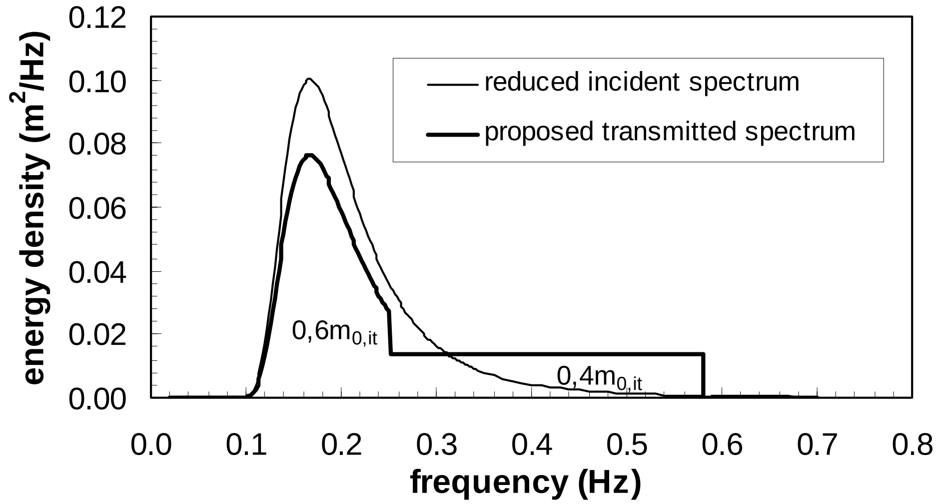

Figure 17. Calculated reduced spectrum and shift of energy resulting in the final transmitted spectrum

Then this total energy is divided and 40% is brought to the higher frequencies, see Figure 17. The division between "long" and "short" energy is taken at 1.5 f_p, in this example at 0.25 Hz. The part of the spectrum with frequencies smaller than 0.25 Hz or 1.5 f_p is similar to the incident spectrum, the total energy is 60% of the total *transmitted* energy. The part of the spectrum with frequencies larger than 1.5 f_p can be described with constant energy up to 3.5 f_p, which means from 0.25 Hz to 0.583 Hz in the example in Figure 17. The bold line in Figure 17 finally shows the transmitted wave spectrum.

Effects on wave run-up and overtopping

The transmitted spectrum has been divided into two parts and can also be treated like that in order to establish wave run-up and overtopping. In fact it can be treated as a bi-modal or double peaked spectrum. See Mendez Lorenzo et al. (2000) for a reference how to deal with double peaked spectra and wave overtopping. The effect will be that less wave overtopping or run-up is expected in comparison to the traditional method, as less energy is present at high periods.

If a certain distance is present between the low-crested structure and the dike, see the situation in Figure 1, local wave generation may play a role too. The effect of the presence of energy especially at high frequencies is that local wave generation by wind can be much faster and higher waves may be expected at the dike than without transmission. In fact the horizontal part in Figure 17 will grow to a second peak by wind.

References

Goda, Y. (1969). Re-analysis of laboratory data on wave transmission over breakwaters. Rep. Port and Harbour Res. Inst., Vol. 8, No. 3, pp. 3-18

Goda, Y. (1985). Random seas and design of maritime structures, Tokyo Press

Lee, D.S, S.W. Park, K.D. Suh and Y.M Oh (1994). Hydraulic experiments for basic design offshore breakwater for protecting artificial island. Proc. Hydro-Port '94, Yokosuka, Japan

Mendez Lorenzo, A.B, J.W. van der Meer and P.J. Hawkes (2000). Effects of bi-modal waves on overtopping: application of UK and Dutch prediction methods. ASCE, proc. 27th ICCE, Sydney, Australia

Raichlen, F., J.C. Cox and J.D. Ramsden (1992). Inner harbor wave conditions due to breakwater overtopping. Proc. ASCE, Coastal Engineering Practice '92. Long Beach, California, US

Tanimoto, K, S. Takahashi and K. Kimura (1987). Structures and hydraulic characteristics of breakwaters – the state of the art of breakwater design in Japan. Report of the Port and Harbour Research Institute, Vol. 26, No. 5

Van der Meer, J.W., 1990. Data on wave transmission due to overtopping. Delft Hydraulics Report H 986

Van der Meer, J.W. and I.F.R. Daemen (1994). Stability and wave transmission at low-crested rubble mound structures. ASCE, Journal of WPC&OE, Vol. 120, No. 1, 1-19

Van Vledder, G.Ph. (1992). Statistics of wave group parameters. ASCE, proc. 23rd ICCE, Venice, Italy. pp. 946-959.

Effects of bi-modal waves on overtopping:
application of UK and Dutch prediction methods

A.B. Mendez Lorenzo[1], J.W. van der Meer[2] and P.J. Hawkes[3]

Introduction and background

Sometimes dike sections or seawalls are partially protected by low-crested structures up to one kilometre in front of these coastal defences and more than one kilometre in length. Wave energy may be transmitted over these low-crested structures or dams and waves can penetrate through various openings. These waves have periods similar to the wave periods of the incident waves. Local wave growth of shorter period waves may become important if some fetch is present between dam and coastal defence. Wave spectra in front of the dike sections are often therefore bi-modal. Also sea and swell and/or irregularly shaped wave generation areas may give rise to these bi-modal or double peaked spectra. Until now, little was known about their influence on required dike heights.

A series of physical model studies (conducted at a nominal scale of 1:20) were undertaken by HR Wallingford for the Flood and Coastal Defence with Emergencies Division of the UK Ministry of Agriculture, Fisheries and Food (MAFF). The intention was to provide information on wave breaking behaviour and the impact of bi-modal wave conditions on beaches and coastal structures. This research was described by Coates et al. (1998) and by Hawkes et al. (1998). Wave conditions and wave overtopping were measured for two or three water levels over different bed slopes of 1:50, 1:20 and 1:10.

During a project for the Dutch Public Works Department - IJsselmeer District, Alkyon and Infram studied wave-structure behaviour over low-crested dams and the effect of bi-modal seas on required dike heights. As a part of this project

[1]Ministry of Transport, Public Works and Water Management, Road and Hydraulic Engineering Division, POBox 5044, 2600 GA Delft, the Netherlands; a.mendezlorenzo@dzh.rws.minvenw.nl
[2]Infram, POBox 81, 3890 AB, Zeewolde, the Netherlands; jentsje.vandermeer@infram.nl
[3]HR Wallingford, Howbery Park, Wallingford, Oxfordshire, OX10 8BA, United Kingdom; pjh@hrwallingford.co.uk

Infram visited HR Wallingford and used above research to establish a method for predicting wave overtopping with bi-modal seas for Dutch applications. The research was described (partly) by Van der Meer et al. (2000a). At that time it was recognised that the wave and wave overtopping data measured by HR Wallingford would be interesting to the Dutch Public Works Department for several reasons as they are responsible for establishment of wave boundary conditions and guidelines for safety assessment of the Dutch coastal defences. The actual work consisted of four parts and was described in full depth in Van der Meer et al. (2000b):

- re-analysis of approximately 200 wave flume runs to obtain various time and frequency domain parameters. This work was performed by HR Wallingford
- validation of the SWAN-model and analysis of wave breaking formulations. This work was performed by Alkyon and Delft Hydraulics
- validation of a model on shallow wave height statistics by Delft Hydraulics
- further analysis on wave overtopping by uni- and bi-modal seas, performed by Infram in co-operation with Delft Hydraulics

Only the latter part, the wave overtopping analysis, is the subject of this paper.

Model tests

Wave overtopping on 1:2 and 1:4 uniform and smooth slopes was measured with 1:50, 1:20 and 1:10 beach slopes, see Coates et al. (1998) and Hawkes et al. (1998). About 40 tests with uni-modal spectra and 90 tests with bi-modal spectra were available with overtopping measurements for both slopes. During calibration tests, without a structure in the flume, the waves were measured along the foreshore.

The model scale used was 1:20 and the data are given in prototype values. In general, significant wave heights varied from 1.5 to 4.4 m with peak periods between 5 and 13 s for the uni-modal tests. The significant wave heights for the bi-modal tests varied between 0.6 and 4.4 m. The shortest peak period of the bi-modal spectrum was always close to 6-7 s. The second peak period ranged from 11 to 21 s. Various parameters in both time and frequency domain were calculated and used for further analysis.

Wave deformation over the beach slope

Spectral changes. Figures 1-3 show the spectra from a few selected tests. Each figure shows the spectrum that was generated and measured offshore of the foreshore slope and the spectrum that was measured at the end of the slope (inshore) which was in fact the location of the toe of the slope of 1:2 or 1:4. These waves, however, were measured during the calibration tests with no structure in the flume.

Figure 1 shows a uni-modal spectrum on a foreshore slope of 1:50. The energy at the peak frequency decreased due to wave breaking and some energy was transformed to longer periods. Figure 2 gives an example of a bi-modal spectrum, also on a slope of 1:50. Due to wave breaking, the low-frequency energy reduced a little (around 0.05 Hz) and generated a second harmonic at 0.10 Hz. The second generated peak at 0.14 Hz did not change. The final result in front of the toe of the slope is a spectrum with three peaks! Figure 3 provides a further example of a bi-modal spectrum with an extremely large difference between the two peaks: 6 and 21 s. On the 1:50 foreshore slope the energy at the long peak period increases due to shoaling, whilst the energy at the short peak period reduces due to wave breaking. The final result is still a bi-modal spectrum, but with altered energy densities at the two peaks.

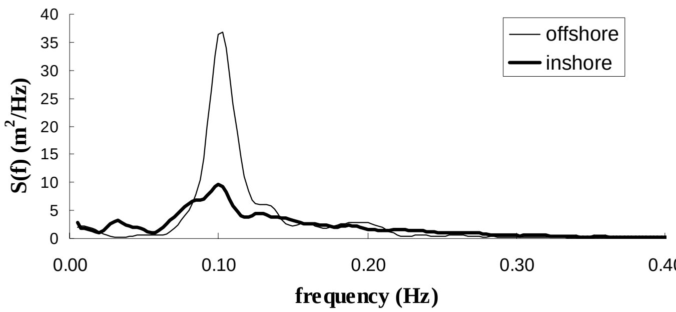

Figure 1. Spectral changes on foreshore slope 1:50; H_{so}=4.4 m and T_p=9.8 s

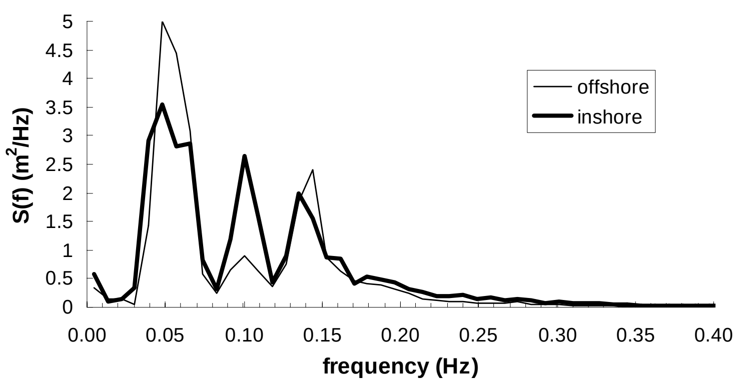

Figure 2. Spectral changes on foreshore slope 1:50; Bi-modal spectrum, H_{so}=1.9 m and T_p=7 and 19 s

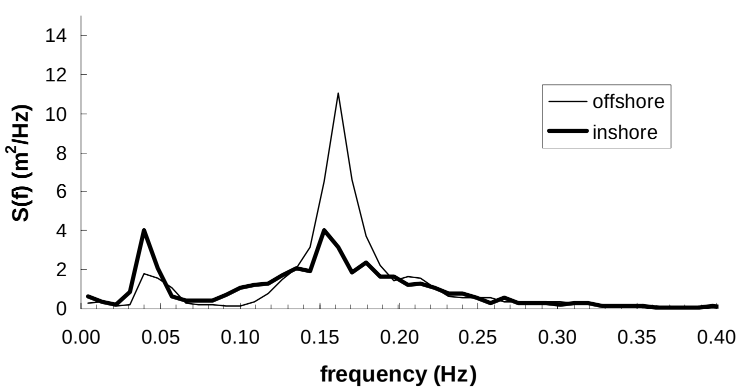

Figure 3. Spectral changes on foreshore slope 1:50; Bi-modal spectrum, H_{so}=2.6 m and T_p=6 and 21 s

It can be concluded that even for uni-modal waves in deep water there may be bi-modal conditions at the toe of the structure. Sometimes the long energy peak is higher than the original peak, shifting the “peak period” drastically. It means that using a peak period at the toe of the structure in overtopping formulae can generate fairly large scatter, simply due to the fact that bi-modal spectra are present. A peak period in deep water could be used for uni-modal spectra, but this ignores the fact that bi-modal spectra may exist at the toe of the structure.

For both uni-modal (breaking) and bi-modal spectra, one peak period is not a sufficient parameter. If the division of energy between the peaks is known, various methods can be used which initially treat the peaks independently and then make an integration. This could even be done for three or more peaks. It would, however, be easier if a spectral period could be chosen, independent of the actual number of peaks. This paper deals with such a spectral period.

Wave breaking. For a few selected tests the wave height evolution along the foreshore has been given in Figures 4-6. The first two figures 4 and 5 give the $H_{1/3}$ along the foreshore for uni-modal waves and different tests. Distance 0 m means at the toe of the structure and positive values are in the offshore direction.

Figure 4 shows the shoaling and breaking on a 1:50 foreshore slope. This slope starts at a distance of 400 m and the water depth at the location of the toe (calibration tests, no structure in the flume!) amounts to 4 m. There is quite some wave breaking for this (small) water depth of 4 m at the toe.

Figure 5 describes the wave breaking on the 1:20 slope with a 6 m water depth at the toe of the structure. Here shoaling and breaking is present over a short distance due to the steep foreshore which starts at a distance of 160 m. The three tests in Figure 5 have more or less the same offshore wave height, but differ in wave period (0f2 means a test with a mean wave steepness of 0.02 and 0f6 with 0.06). The long period test with a mean wave steepness of 0.02 shoals from an offshore wave height $H_{1/3}$=3.8 m to a maximum value of $H_{1/3}$=5.4 m just before breaking!

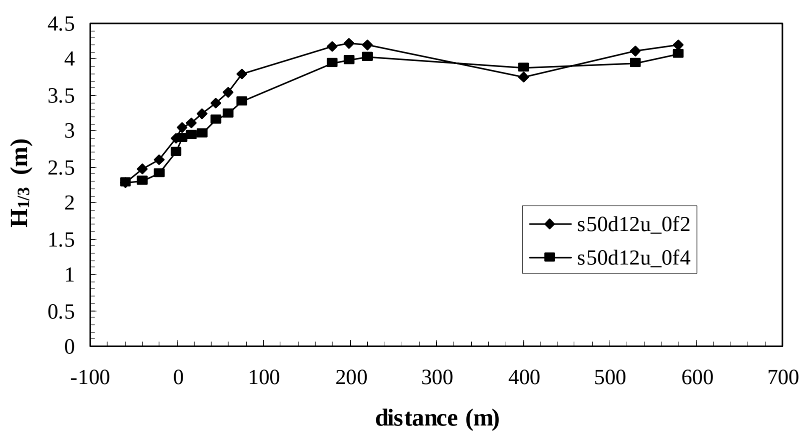

Figure 4. Wave height deformation on a foreshore slope of 1:50. Water depth at the location of the toe 4 m; uni-modal waves

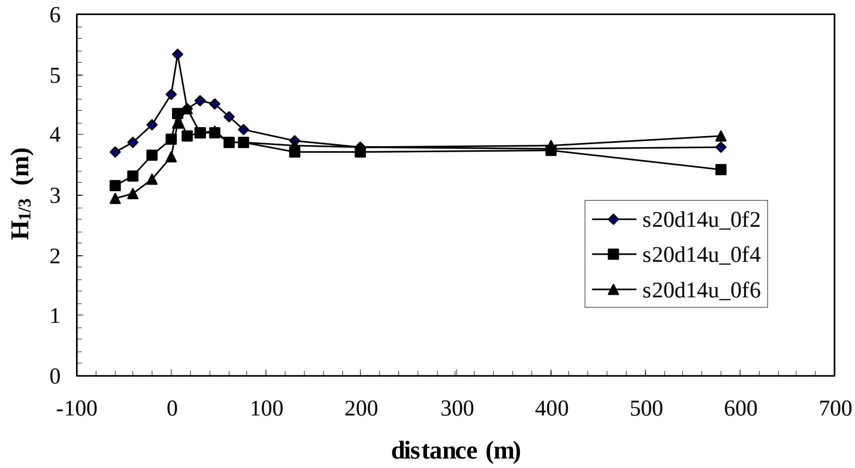

Figure 5. Wave height deformation on a foreshore slope of 1:20. Water depth at the location of the toe 6 m; uni-modal waves

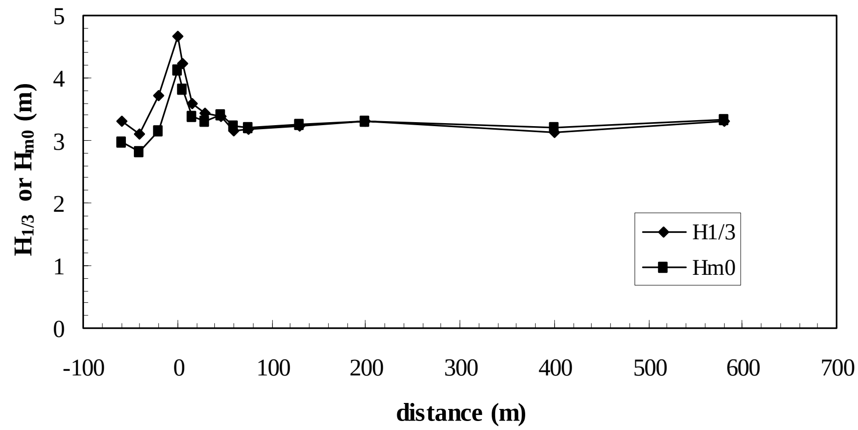

Figure 6. Wave height deformation on a foreshore slope of 1:10. Water depth at the location of the toe 6 m; bi-modal waves

The graph shows that the actual location chosen for the wave height from which to estimate the overtopping rate is quite important. A little shift in location around the toe may result in a significant higher or lower wave height.

Figure 6 gives the behaviour of bi-modal waves on a foreshore slope of 1:10. This slope starts offshore at a distance of 80 m. Now only one test is shown and for this test both the $H_{1/3}$ and H_{m0}. Bi-modal waves show a similar behaviour to uni-modal waves. In the wave breaking area generally the H_{m0} is smaller than the $H_{1/3}$, which can be expected. In *deep water* both the spectral wave height H_{m0} and the statistical wave height $H_{1/3}$ have more or less the same value. In that sense it does not matter which wave height is used in wave overtopping calculation.

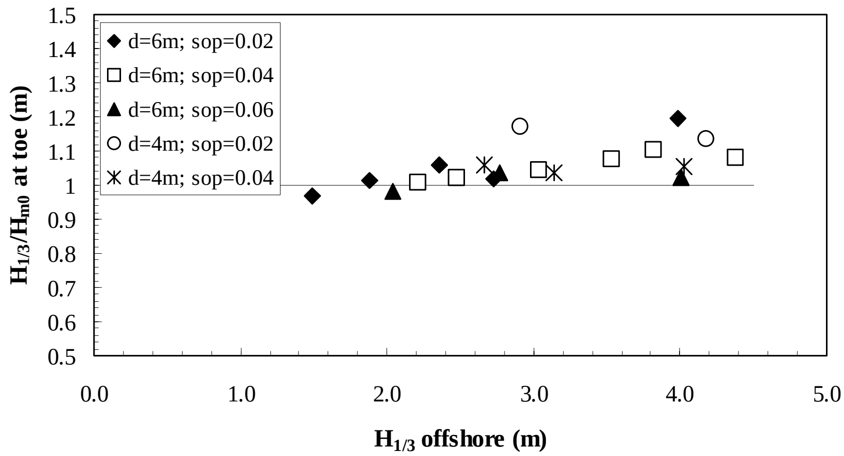

Figure 7. The breaking ratio $H_{1/3}/H_{m0}$ at the location of the toe of the structure during calibration tests. Foreshore slope 1:50, uni-modal tests

Figure 7 gives the $H_{1/3}/H_{m0}$ ratio for all the uni-modal spectra on a foreshore slope of 1:50, the horizontal axis being the $H_{1/3}$ in deep water. The larger the offshore wave height the more wave breaking may be expected and therefore a larger ratio may be expected. This is indeed the case in Figure 7, where for lower wave heights around 2 m a ratio of 1 is found and for larger wave heights a ratio larger than 1. This figure also clearly shows that the ratio increases with decreasing wave steepness. Both tests with the lowest steepness of 0.02 give clearly the largest ratio.

It can be concluded that for steep slopes the location where the wave height is taken to be responsible for the wave overtopping, is quite critical due to the significant changes within a short distance. Furthermore it can be concluded that the spectral and statistical wave height may differ substantially.

Wave periods. A spectral wave parameter close to the peak period (for uni-modal waves) would be preferred as it was proven earlier that a longer period than the mean period may account for differences in spectral shape. Such spectral wave periods are T_{m-10}, T_{m-20} and T_{m-2-1}, where $T_{m\ x1\ x2}=m_{x1}/m_{x2}$ with m_{xx} the frequency moment of the wave spectrum. For a given theoretical spectral shape there is a fixed relationship with the peak period, given in Table 1.

Table 1. Relationship T_p/T_{mx1x2}

	Jonswap	*Pierson Moskowitz*
T_{m-2-1}	1.06	1.08
T_{m-20}	1.08	1.12
T_{m-10}	1.11	1.17
T_{m01}	1.21	1.30
T_{m02}	1.30	1.40

The periods with negative moments give more weight to the energy at the lower frequencies. Due to wave breaking, quite some energy was generated at the toe of the structure, which will tend to increase the first mentioned wave periods in Table 1. In Van Gent (1999) the performance of these wave periods was analysed numerically and it was concluded that the wave period T_{m-10} is the optimal wave period for describing wave run-up and wave overtopping for non uni-modal spectra. And also in Van Gent (2000) this conclusion was confirmed based on physical model tests with wave run-up and wave overtopping.

Wave overtopping

Problem definition. A lot of research on wave overtopping has been performed in (recent) decades. Most of the resulting prediction formulae are based on model tests with not too much wave breaking and with uni-modal waves offshore. The above analysis of wave deformation on foreshore slopes, including bi-modal wave spectra, showed that $H_{1/3}$ and H_{m0} at the toe of the structure may differ [comma] and that a spectral period may be preferred above a peak period. There are various possibilities for the choice of a spectral peak period.

The best choice of parameter would be that which gives the closest agreement with the existing formulae, as in that case there would be no need to develop a new formula with a transition to the existing ones. (This under the requirement that the scatter would be similar as for other choices, and preferably the lowest.)

Overtopping formulae. Two of the main overtopping formulae will be considered here for evaluation against the test data. These are the formula of Owen (1980) and the TAW formulae (Van der Meer et al., 1998).

Owen:

$$\frac{q}{\sqrt{gH_s^3}}\sqrt{\frac{s_m}{2\pi}} = A\exp\left(-B\frac{R_c}{H_s}\sqrt{\frac{s_m}{2\pi}}\right) \qquad (1)$$

TAW:

$$\frac{q}{\sqrt{gH_s^3}}\sqrt{\frac{s_{op}}{\tan\alpha}} = 0.06\exp\left(-5.2\frac{R_c}{H_s}\frac{\sqrt{s_{op}}}{\tan\alpha}\right) \qquad (2)$$

with maximum: $$\frac{q}{\sqrt{gH_s^3}} = 0.2\exp\left(-2.6\frac{R_c}{H_s}\right) \qquad (3)$$

with:

q	= average overtopping discharge	m^3/s per m width
g	= acceleration of gravity	m/s^2
H_s	= significant wave height, $H_{1/3}$ or H_{m0}	m
s_m	= wave steepness with mean period T_m	-
R_c	= crest freeboard	m
s_{op}	= wave steepness with peak period T_p	s
$\tan\alpha$	= slope angle	-

Table 2. A and B coefficients in the Owen formula (equation 1)

Slope	A	B
1:1	7.94×10^{-3}	20.1
1:1.5	8.84×10^{-3}	19.9
1:2	9.39×10^{-3}	21.6
1:2.5	1.03×10^{-2}	24.5
1:3	1.09×10^{-2}	28.7
1:3.5	1.12×10^{-2}	34.1
1:4	1.16×10^{-2}	41.0
1:4.5	1.20×10^{-2}	47.7
1:5	1.31×10^{-2}	55.6

A and B are coefficients in the Owen formula (equation 1) given for each slope (slopes of 1:1; 1:2; and 1:4 were measured, for other slopes an interpolation was performed). The coefficients were slightly changed later on by HR Wallingford and are given in Table 2. In fact the Owen formula was developed further during the TAW-work (around 1990) when Owen's original data were re-used. The main differences or developments were:

- include $\tan\alpha$, as this will lead to one set of formulae instead of a table of coefficients for distinct slopes
- change to T_p, as it was found that a longer period than T_m gave similar results for different spectral shapes, where T_m gave deviations
- include a maximum for non-breaking waves. It was found that there was no or hardly any influence of $\tan\alpha$ and T_p if the waves did not break on the slope.

The TAW formulae also include reduction factors for roughness, berms, oblique wave attack, and walls on top of a dike. As this paper deals with uniform slopes only, these factors (which can also be applied to the Owen formula) will not be treated here.

There is another difference between the Owen and TAW formulae. Owen (1980) gives a figure for the breaking index of the wave height in shallow water. Actually, one should take the significant wave height and mean period at deep water, apply the figure with the breaker index and apply the resulting wave height in the formula. The TAW formulae were mainly based on relatively deep water waves and the wave height to be used is the wave height at the toe of the structure. This implies that one should have a method available to predict this wave height at the toe of the structure.

Analysis of wave overtopping. The TAW formulae consider breaking and non-breaking waves on a slope. For non-breaking waves there is no influence of slope angle or wave period , but only of wave height and crest freeboard (equation 3). The test series include long periods that give non-breaking conditions for the 1:4 slope. At the 1:2 slope the conditions are always non-breaking. This means that in tests where waves are non-breaking on both slopes, the wave overtopping can be compared directly. Figure 8 gives these data.

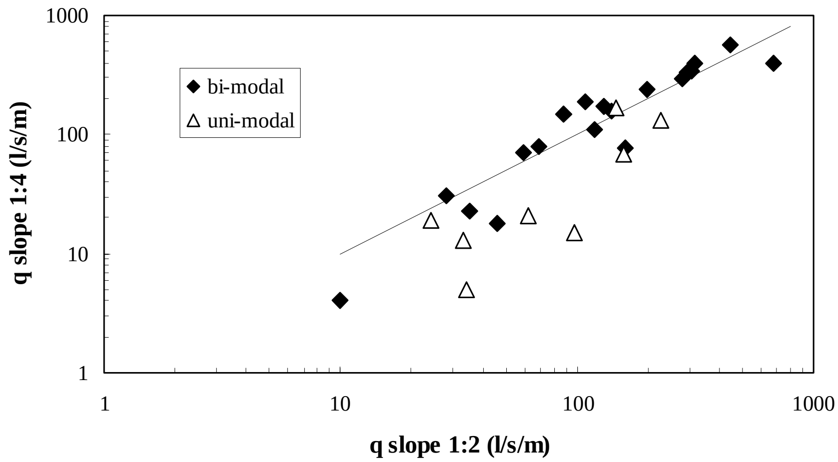

Figure 8. Direct comparison of wave overtopping for 1:2 and 1:4 slopes for non-breaking waves on the slope

For the uni-modal tests, generally the 1:2 slope gives more overtopping than the 1:4 slope, especially for lower overtopping rates. The bi-modal tests, however, show a clear correlation between the two slopes, supporting the conclusion that there is hardly any influence of slope angle on wave overtopping for non-breaking conditions. At present there is no explanation as to why uni- and bi-modal tests give different results.

Figures 9 and 10 give the measurements together with the predictions by Owen, equation 1 (together with the original data of Owen). Here the $H_{1/3}$ at the toe of the structure was taken together with T_m in deep water.

Figure 9 gives the results for the slope of 1:2. The bi-modal waves show more scatter than the uni-modal waves. This can be expected as the mean period, instead of a larger period, will increase the scatter for different spectral shapes, which occur

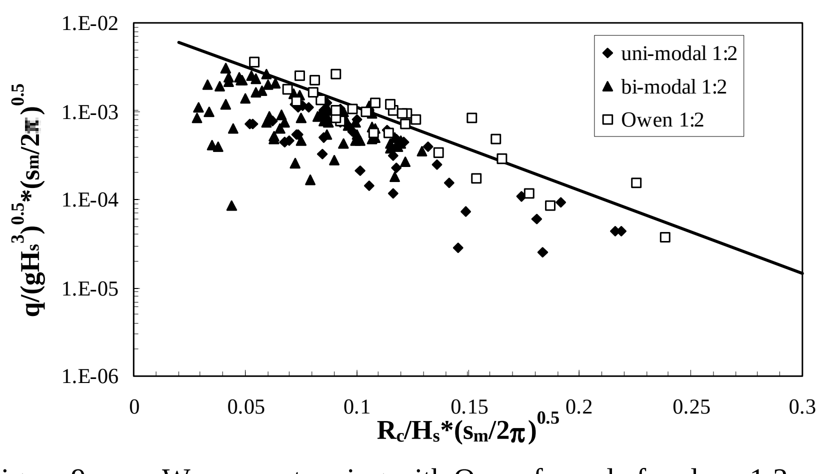

Figure 9. Wave overtopping with Owen formula for slope 1:2

particularly in the case of bi-modal waves. Moreover, the average trend gives less overtopping than predicted by Owen. This may partly be explained by the presence of longer wave periods than were used in development of the formula, but actually have no or minor influence. Still the deviation between measurements and predictions is quite large, especially for the uni-modal waves, although it is reassuring to note that the original data of Owen lie close to the line.

Figure 10 gives the data, together with the Owen formula for the slope of 1:4. Here the data are around the line, with more scatter for the bi-modal spectra, which can be expected as the mean period has been used to characterise the bi-modal spectrum.

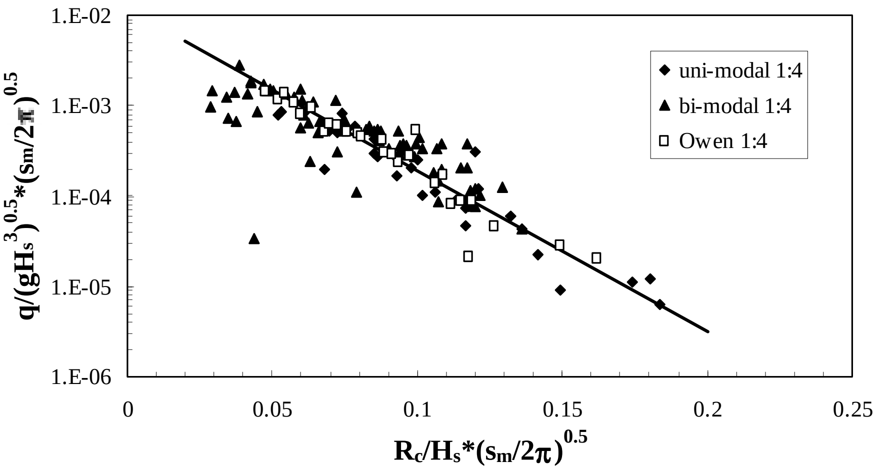

Figure 10. Wave overtopping with Owen formula for slope 1:4

It can be concluded that the steep slope of 1:2 shows a deviation from the predicted line. For both structure slopes the bi-modal spectra are not well described by the mean period, as the scatter is larger than for uni-modal waves.

For the TAW formulae (equations 2 and 3) various definitions of wave height and wave period were used. The data were plotted with $H_{1/3}$ or H_{m0} at the toe of the structure in combination with T_{m-10}, T_{m-20} or T_{m-2-1}, also measured at the toe of the structure. As shown in Table 1 there is a difference between the peak period and the spectral wave parameters. The spectral wave parameters for uni-modal waves are normally a little smaller than the peak period. For an objective comparison one should include the spectral wave period in the prediction. For simplicity it is assumed that a Jonswap spectrum represents most of the earlier tests in deep water, and therefore the following relationships were used to modify the TAW formulae or the prediction lines in the figures: $T_p = 1.11\ T_{m-10} = 1.08\ T_{m-20} = 1.06\ T_{m-2-1}$.

Not all the graphs can be given in this paper. After thorough analysis the final conclusion is that the data support the use of $H_{1/3}$ and T_{m-10} at the toe of the structure, which is consistent with conclusions mentioned earlier by Van Gent (2000). Only the graphs with these parameters are given here. Figure 11 shows the data for breaking waves, together with equation 2, adapted for use of T_{m-10} by using a factor T_p=1.11T_{m-10}. The data show the same trend as the line, but are on average a little

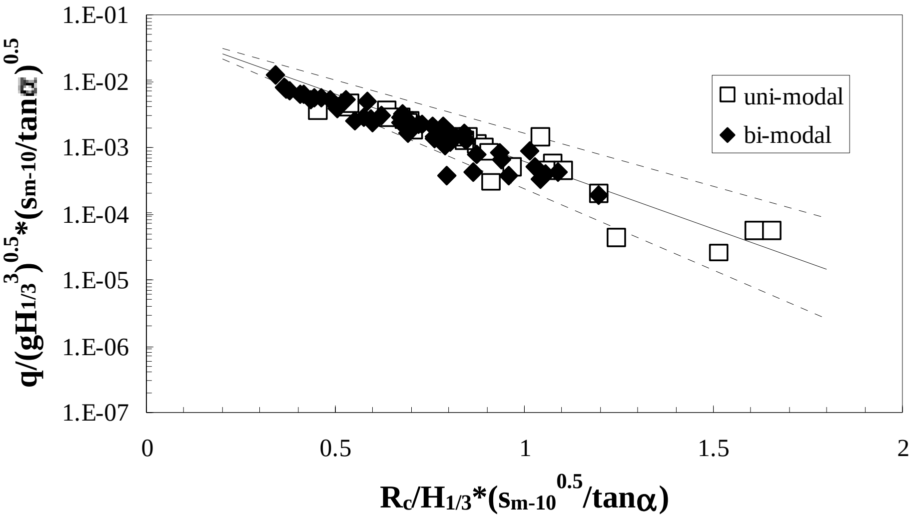

Figure 11. Wave overtopping data with TAW formula for breaking waves (equation 2) with the use of $H_{1/3}$ and T_{m-10} (the best choice)

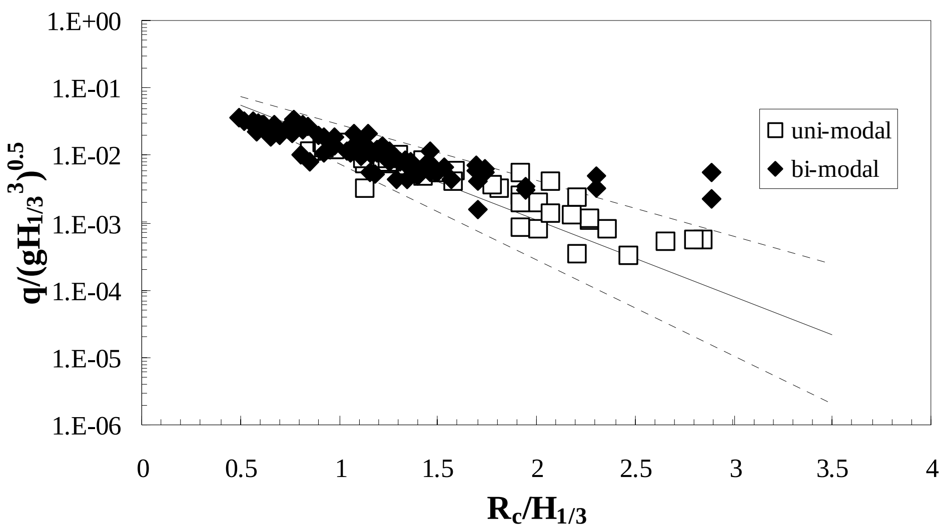

Figure 12. Wave overtopping data with TAW formula for non-breaking waves (equation 3) with the use of $H_{1/3}$ (and T_{m-10} for definition of breaking or non-breaking)

lower than this line, certainly for larger overtopping rates. This suggests a slightly conservative prediction method, but the differences are small.

Figure 12 shows the data for non-breaking waves on the slopes. On average the data are present around the line, but the data shows less overtopping for larger discharges and more overtopping for smaller discharges (the right side of the graph). It appears that the trend should be gentler than given by the prediction line. In fact the same was found with the original data of Owen (1980) for slopes 1:1 and 1:2, but together with data from other sources, the average line is closer to the equation, see for instance Van der Meer et al. (1998).

For application of the TAW formulae, preference should be given to the use of $H_{1/3}$ and T_{m-10} for non-uni-modal wave spectra (bi-modal, more peaks or a wide spectrum due to wave breaking). This conclusion holds only for not too severe wave breaking (say not more than 50% reduction in wave height by breaking) and fairly steep foreshore slopes. Very severe wave breaking on gentle foreshores has been described by Van Gent (2000) and may include the effects of surf beat, resulting in increased wave overtopping. For application of the TAW formulae, $T_p = 1.11\ T_{m-10}$ should be used. (An alternative would be to rewrite the TAW formulae with T_{m-10} instead of T_p.)

Application of results

Scientific approach. Analysis thus far has focussed on the use of a spectral wave period which includes all kinds of spectral shapes. This has resulted in the conclusion to use T_{m-10} in the TAW formulae with a correction factor between T_p and T_{m-10}. The approach can be summarised as follows:

- Establish $H_{1/3}$ and T_{m-10} at the toe of the structure
- Use $T_p = 1.11\ T_{m-10}$
- Use the TAW formulae

This approach is called a scientific approach as it is still fairly complicated to establish the correct T_{m-10}. SWAN is not able to predict this period. First research shows (Van Gent and Doorn, 2000) that Boussinesq type models may be able to do this, but these type of models are still in use mainly by researchers and are not available for most practising engineers. The measurements in the tests give directly the desired wave period and height at the toe of the structure. Figure 13 shows the predicted against measured overtopping discharges for the slope 1:4, using the measured wave heights and periods at the toe for the predictions.

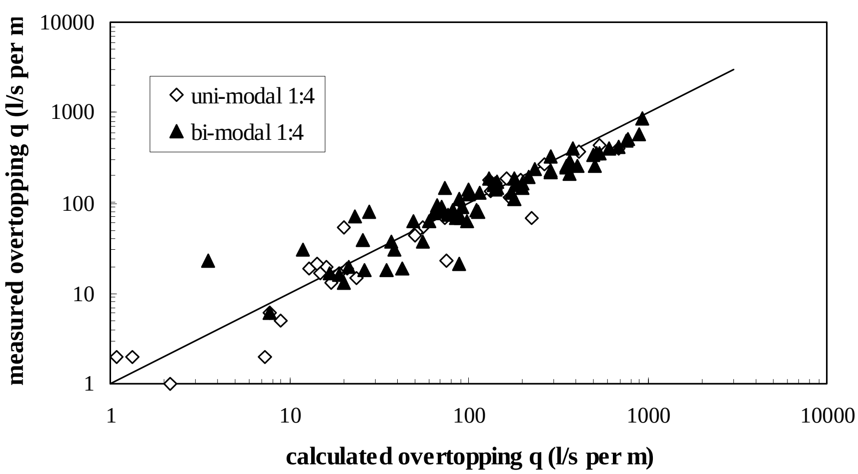

Figure 13. Scientific approach: use of $H_{1/3}$ and T_{m-10} at toe of structure; all data on slope 1:4; measured overtopping versus predicted

In Figure 13 only data for a slope of 1:4 have been plotted. Results for the 1:2 slope are comparable both for uni- and bi-modal waves, for the scientific approach as well as for the practical approach described below, as in each approach the maximum overtopping discharge for non-breaking waves is reached, which means that there is no influence of wave period.

Practical approach. Most standard methods for estimation of overtopping rate under uni-modal wave conditions are based on the use of a single offshore wave height and wave period. A potential problem arises if the spectrum becomes bi-modal before arrival at the structure where (at least) two peak periods may then be present. Bearing in mind that the offshore spectrum is often known, either from measurements or predictions, a simple approach was suggested by HR Wallingford (Hawkes et al., 1998) using the two (or more) separate offshore periods in separate overtopping predictions, before combining them into a single overall prediction. This idea was developed further and provides the basis for the practical approach given here. The method for bi-modal spectra can be summarised as follows:

- Establish the peak periods of both peaks *offshore,* T_{p1} and T_{p2}, with corresponding wave heights H_{s1} and H_{s2}, being the spectral wave heights $4\sqrt{m_{01}}$ or $4\sqrt{m_{02}}$ *offshore*
- Establish H_{m0} at the toe of the structure with a (simple) energy model
- Calculate $H_{1/3}$ using H_{m0} above by the method described in Battjes and Groenendijk (2000)
- Calculate breaker parameters ξ_{op1} and ξ_{op2} with respectively T_{p1} and $H_{1/3}$ and T_{p2} and $H_{1/3}$, where $\xi_{op}=\tan\alpha/\sqrt{2\pi H_s/(gT_p^2)}$
- Calculate the equivalent breaker parameter:
  $$\xi_{op}(eq) = (\xi_{op1} H_{s1}^2 + \xi_{op2} H_{s2}^2)/(H_{s1}^2 + H_{s2}^2) \tag{4}$$
- Calculate the overtopping discharge for with equation 2 and 3, using $\xi_{op}(eq)$.
- Equation 2 can be rewritten to:
  $$\frac{q}{\sqrt{gH_s^3}} = 0.06\xi_{op}/\sqrt{\tan\alpha}\exp\left(-5.2\frac{R_c}{H_s}\frac{1}{\xi_{op}}\right) \tag{5}$$

This is called the practical approach as the (bi-modal) wave spectrum offshore is used, and a simple model to predict the wave height at the toe of the structure. Figure 14 gives the calculated and measured overtopping discharges for this approach, which can directly be compared with the results of the scientific approach, Figure 13.

Comparison of the two figures results in the following conclusion: the 1:4 slope with uni-modal spectra shows a slightly smaller scatter for the practical approach than for the scientific approach. The 1:4 slope with bi-modal spectra is slightly better predicted by the scientific approach as the practical approach gives mainly under predictions for small overtopping discharges. In general it can be concluded that the practical approach does not differ much from the scientific approach for the situations which were considered here, ie not too much wave breaking and fairly steep foreshores.

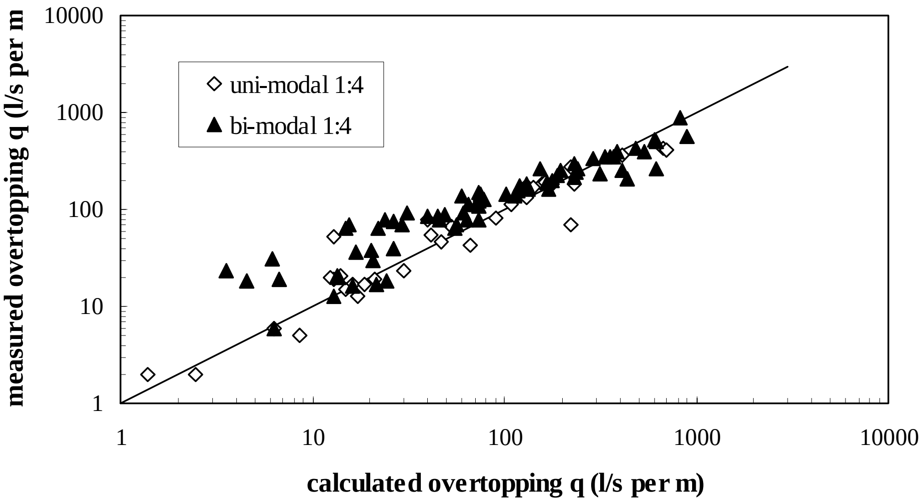

Figure 14. Practical approach: use of $H_{1/3}$ at the toe and peak periods offshore; all data on slope 1:4; measured overtopping versus predicted

References

Battjes, J.A. and H.W. Groenendijk (2000). Wave height distributions on shallow foreshores. Journal of Coastal Engineering, Volume 40, Number 3, 161-182

Coates, T.T., R.J. Jones and P. Bona (1998). Wave flume studies on responses to wind/swell and steep approach slopes. Research Report TR 24, HR Wallingford

Hawkes, P.J., T.T. Coates and R.J. Jones (1998). Impact of bi-model seas on beaches and control structures. Research report SR 507, HR Wallingford

Owen, M.W. (1980). Design of seawalls allowing for wave overtopping. Hydraulics Research Station, Report No EX 924

Van der Meer, J.W., P. Tönjes and J.P. de Waal (1998). A code for dike height design and examination. Coastlines, Structures and Breakwaters. ICE, pp. 5-19. Editor N.W.H. Allsop, Thomas Telford, London, UK

Van der Meer, J.W., E. Regeling and J.P. de Waal (2000a). Wave transmission: spectral changes and its effect on run-up and overtopping. ASCE, Proc. 27th ICCE, Sydney, Australia

Van der Meer, J.W., D.P. Hurdle, G.Ph. van Vledder, M.R.A. van Gent and R.C. Ris (2000b). Uni- and bi-modal wave spectra on steep foreshores. Validation of the SWAN-model, wave height statistics and wave overtopping, based on HR Wallinford data. Report i230 / A509 / H3510 of Infram, Alkyon and Delft Hydraulics

Van Gent, M.R.A. (1999). Wave run-up and wave overtopping for double-peaked wave energy spectra. Delft Hydraulics Report H3351, January 1999, Delft

Van Gent, M.R.A. (2000). Wave run-up on dikes with shallow foreshores. ASCE, Proc. 27th ICCE, Sydney, Australia

Van Gent, M.R.A. and N. Doorn (2000). Numerical model investigations on coastal structures with shallow foreshores. Delft Hydraulics Report H3351, Delft